

# The reinforcement learning-based multi-agent cooperative approach for the adaptive speed regulation on a metallurgical pickling line

Anna Bogomolova

*Severstal Digital*

Moscow, Russia

aiu.bogomolova@severstal.com

Kseniia Kingsep

*Severstal Digital*

Moscow, Russia

ka.kingsep@severstal.com

Boris Voskresenskii

*Severstal Digital*

Moscow, Russia

bs.voskresenskii@severstal.com

**Abstract**—We present a holistic data-driven approach to the problem of productivity increase on the example of a metallurgical pickling line. The proposed approach combines mathematical modeling as a base algorithm and a cooperative Multi-Agent Reinforcement Learning (MARL) system implemented such as to enhance the performance by multiple criteria while also meeting safety and reliability requirements and taking into account the unexpected volatility of certain technological processes. We demonstrate how Deep Q-Learning can be applied to a real-life task in a heavy industry, resulting in significant improvement of previously existing automation systems. The problem of input data scarcity is solved by a two-step combination of LSTM and CGAN, which helps to embrace both the tabular representation of the data and its sequential properties. Offline RL training, a necessity in this setting, has become possible through the sophisticated probabilistic kinematic environment.

**Index Terms**—smart manufacture, Deep-reinforcement learning, CGAN, control systems

## I. INTRODUCTION

Machine Learning (ML) today has become an essential part of digital transformation in industry. Its methods find broad practical application in such a complex class of problems, as predictive maintenance, quality verification (image recognition) and quality prediction [1]. However, despite the fact that the traditional ML approach allows to significantly improve certain areas of manufacturing process, that approach is usually fixed in the conditions applied and can not immediately response to the changes raised in the environment. This situation is more obvious in prediction tasks, when predicted poor quality of the object requires some actions to be taken to prevent an undesirable result. In industry, where most of ML approaches applied to the mechanisms of continuous action with hundreds or more sensors, the evaluation of regulation strategy is becoming a non-trivial task. An additional complication arises from the already mentioned continuous character of action in manufacturing lines. The high frequency of consecutive events requires the regulation response to be applied with at least the same periodicity. Meaning all of the above, the methods of prescriptive analytics, such as Reinforcement Learning (RL) algorithms, could be considered as a more suitable approach for application in industry.

The main advantage of RL comes from the ability to construct many potential scenarios considering different actions applied to the system and to give analytical evaluation to each of them [2]. Moreover, it also allows to assess a long-term effect of consequently taken actions. The combination of such properties attracts significant interest to the RL framework in the fields where predictions from ML algorithms are applied with special caution, due to potential consequences of their implication to the local environment (healthcare [3], risk management [4], network traffic control [5] and industry [6]).

In this article we report a successful implication of the RL algorithm to the production process on a metallurgical pickling line for the productivity increase problem. Pickling line is a continuously-acting line where steel strips processed in a hot-rolling mill are exposed to removal of iron oxides from their surface. To make the process to be endless, the steel strips are first welded lengthwise at the outlet of the first transport unit (FTU) then fed through a pickling bath (the second transport unit, STU) and finally cut down at the inlet of the third unit (TTU) [7] (Figure 1). While the FTU and TTU have two states of action, "move" or "stop" (to make the welding or cutting process to be possible), the STU has to be always in motion, because the line stoppages lead to steel defects. Therefore, for a smooth work of the whole pickling line the speed regulation of the STU is the most critical issue. Thus, we formulate our problem as a continuous optimization task with the maximization of an average STU's speed over the long run as the main objective. In opposition to the number of publications [8], [9], we consider that the sequence of steel strips entering the pickling line is fixed (production requirement), therefore, we control only the speed of the STU and do not solve the scheduling problem. Moreover, we also focus our attention on the production component of the problem rather than on the chemical one [10], [11], and therefore suppose, that the technological requirements to the pickling speed are satisfied by applying a batch of fixed constraints.

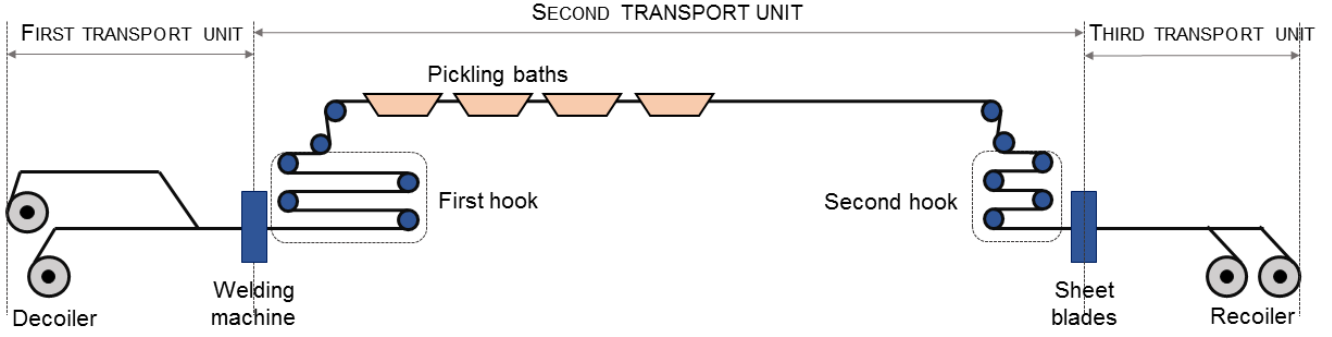


Fig. 1. Scheme of pickling line

## II. PROCESS AND PROBLEM DESCRIPTION

In Figure 1 the scheme of the pickling line is presented. The movement of a steel sheet in two units, the FTU and the TTU is characterized by clear periodicity. That periodicity is determined by the length of a particular sheet. All steel strips processed on the pickling line come in a rolled state. As soon as the head of a new sheet is welded with the tail of the previous one, the unrolling process starts. The FTU moves evenly and then slows down when the sheet length left in the decoiler becomes sufficiently small (that is defined by lines settings). When the unrolling process is finished the welding process starts, and during it the whole FTU is immovable. Then the process repeats for the next roll. The same is fair for the TTU, where instead of the welding process the cutting process takes place, and instead of residual length in the decoiler a residual length before sheet blades is used. The duration of the welding or cutting stages has some variability, but can be predicted with certain errors.

The continual movement of STU becomes possible due to the presence of two hooks, one between the FTU and the STU, the other one between the STU and the TTU and due to a separate operation of every unit. The amount of steel stored in every hook is controlled by the speed difference of the units. The excess in speed of the FTU over the STU results in the fact that the amount of steel entering the first hook is higher than the amount of steel exiting it. Thus, the hook grows in volume to the resulting difference. While the welding stage is running, the excessive amount of steel stored in the hook can be utilized for uninterrupted movement. The opposite situation is for the STU and TTU. When the cutting stage takes place, the amount of steel processed during the stage is stored in the second hook. Then, the excessive amount of steel is reduced in the following stage by applying the speed of the TTU higher than the STU speed. The hooks are limited in capacity (have lower and upper bounds) and the capacity of the second hook is lower than the capacity of the first one. When the amount of steel stored in the first hook approaches the upper bound (or the lower bound for the second hook) the speed of the consequent unit is forced to the speed of the STU. At the

same time the crossing of the opposite boundary can lead to the long downtime.

Therefore, we formulate the entire problem as follows:

- parameters:  $L_f$  - roll length, unrolled in FTU;  $L_t$  - roll length, recoiled in TTU;  $v_f$  - speed of FTU;  $v_t$  - speed of TTU,  $t_W$  - welding time and  $t_C$  - cutting time;

$$t_f = \frac{L_f}{v_f} + t_W \quad \text{and} \quad t_t = \frac{L_t}{v_t} + t_C \quad (1)$$

- decision variable:  $v_s$  - speed of STU,

$$v_s \leq \min(v_{s,set}^1, \dots, v_{s,set}^n) \quad (2)$$

, where  $v_{s,set}^i$  - upper speed boundary for every particular roll, defined manually, and  $n$  - rolls, currently on pickling line;

- constraints:

$$V_f^{min} < \sum_{i=1}^{t_f} (v_{f,i} - v_{s,i}) \quad (3)$$

$$\sum_{i=1}^{t_t} (v_{f,i} - v_{s,i}) < V_s^{max} \quad (4)$$

, where  $V_f^{min}$  - boundary for the first hook;  $V_s^{max}$  - boundary for the second hook;

- objective function:

$$\text{maximize} \sum_{i=1}^n v_{s,i}, n \rightarrow \infty \quad (5)$$

## III. SOLUTION APPROACH

### A. Scheme of solution

The general scheme of the problem solution is shown in Figure 2. There are two principal parts in our approach: the environment reflecting the dynamics of the pickling line and the agent making the decision on the action to be taken.

We developed a three-level environment with each level describing some particular elements of the system. The first level represents the steel strips entered the line. The GANs (Generative Adversarial Network) have been used to simulate

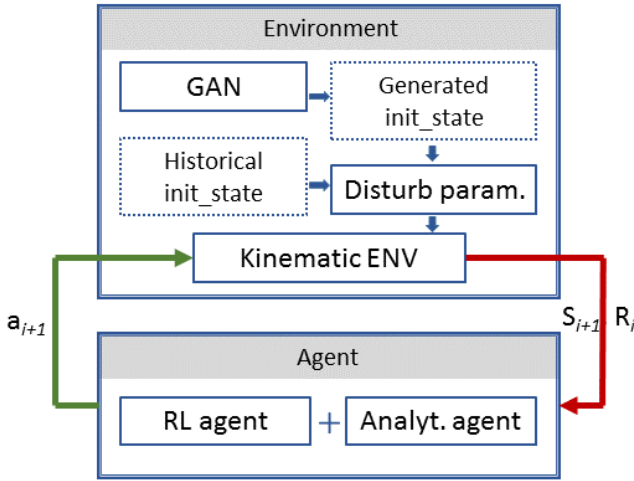


Fig. 2. Scheme of solution

the real sequence of processed strips. The second level can be associated with the disturbance introduced by steel strips to the production mechanisms. That disturbance arises mainly from the variance in geometrical parameters of the strips and could be modeled by using the probabilistic approach. Finally, the third level (Kinematic ENV) characterizes the entire dynamic of the line in accordance with the principles described in the "Process and Problem Description" part. Methods of mathematical modeling have been exploited to simulate the behavior of separate units and to get a highly interpretable scheme of mutual influences.

We also used a two-step agent, consisting of a conservative agent and a RL (reinforcement learning) agent. By the conservative agent (*C-Agent*), we understand the analytical solution of problem evaluated at every step of the production process. To build the RL-agent, various deep RL algorithms were examined.

Hereinafter, we concentrate our attention on two parts of the approach, the development of the GAN algorithm producing the realistic tabular data characterizing the steel sheet parameters and the investigation of the RL algorithm enabled to improve the solution suggested by the conservative agent.

### B. GAN: Input data generation

The training and validation of a reinforcement learning multi-agent system requires a significant amount of input data that was not possible to acquire from real datasets. In our case, the input data represent steel strip characteristics of the metal passing through the pickling line. However, there was available a medium-sized historical dataset only, which could be either augmented or fed to a generative adversarial network (GAN).

Since GANs were introduced [12], their applications initially emerged in the tasks involving synthetic image generation and augmentation [13], [14]. The homogeneous structure of images made them perfect objects for this pioneering

approach, but recently the increasing number of researchers have been using GANs to create data of different structure, including time series, audio, video [15]–[17] and tabular data. For instance, GANs were successfully implemented to augment healthcare records [18]. Xu et al. used a Tabular GAN to generate tabular data with mixed variable types, using preliminary a Gaussian Mixture model for multi-modal columns and a long-short term memory network (LSTM) as a generator [19], or a Conditional Tabular GAN to model rows of data with discrete and continuous columns [20]. Thus, in order to produce realistic synthetic data and to avoid limitations on the size of synthesized dataset, we have chosen to use GANs.

For each epoch of the reinforcement learning multi-agent system training, we required a short sequence of steel strips with certain parameters, thus the task was to produce batches of steel strip characteristics of length 15-20. The realistic sequence of steel strips is crucial in this task, because timings of different technological processes vary from strip to strip depending on their parameters and on the combination of parameters of the adjacent pair of strips. Table I shows the key parameters of the steel strip.

Steel grade is a category of steel comprising its chemical and mechanical properties and other parameters that are directly or indirectly conditioned on the steel grade, thus we have chosen to use a CGAN architecture to generate numerical parameters for this task and to use steel grade as a conditioning parameter. Therefore, we design a two-phase approach to model tabular data with sequential properties.

1) *Steel grade generation with RNN*: Firstly, we generate a sequence of steel grades using a LSTM (Long short-term memory) recurrent neural network [21]. We have chosen this architecture because the parameter behaves as a sequence and can be generated using classical sequence generation approaches. Steel strips with the same parameters: grade, width, thickness - are usually organized in batches of different length during pickling and are pickled consequently. The size of the batch depends on the steel grade, for rare specialized grades the batches are usually smaller. Moreover, there might be consequential batches of the same steel grade, but with different other parameters. Thus, we add an "END" token to the vocabulary of unique steel grades to denote the end of the batch. In this model called GradeGenerator we used a single LSTM layer with 512 units, a dropout layer, a dense layer with softmax activation for the final output and trained on batches of size (*batchsize, timesteps, seqlength*) for 500 epochs optimizing the cross-entropy loss. A smaller number of hidden units turned out to be insufficient to capture specific patterns. We use the batch size of 256 and 20 time steps and do not use an Embedding layer as the size of the unique steel grades vocabulary is relatively small, about 100. Then we sample novel sequences of steel grades according to the softmax distribution to make the results more diverse.

2) *Conditional generative adversarial net (CGAN) for numeric parameters*: After that, we apply a conditional adversarial network algorithm using steel grade from GradeGenerator as an input. The Generative adversarial network consists of

TABLE I  
BASIC STEEL STRIP PARAMETERS

Parameter	Characteristics
Steel grade	Categorical, over 100 unique values, highly imbalanced. Sequential properties are of great importance.
Original width	Integer. Sequential properties are of great importance the difference between consequential strips widths matters.
Resulting width	Integer. Depends on original width that might be adjusted on the pickling line.
Thickness	Integer. Sequential properties are of great importance, there are limitations on thickness differences for adjacent strips.
Weight	Integer, continuous.
Coiling temperature	Float, continuous.
Number of strips in resulting coil	Float. Strips may be rearranged to different coils on the pickling line.

two neural networks: a generator  $G(x)$  that creates data and a discriminator  $D(x)$  that tries to distinguish generated data from real data. Both are trained simultaneously through a minimax game. The discriminator tries to maximize the objective while the generator tries to minimize it, i.e to fool the discriminator by generating realistic samples. The generator uses the feedback provided by the discriminator to synthesize more and more believable samples. For the CGAN the loss is modified and the distributions of the variables are conditioned on  $y$ , in our case it is the steel grade  $Gr$  resulting in the following objective function:

$$\min_G \max_D V(D, G) = \mathbb{E}_{x \sim p_{data}(x)} [\log D(x|y)] + \mathbb{E}_{z \sim p_z(z)} [\log(1 - D(G(z)|y))] \quad (6)$$

The generator takes as an input the Gaussian noise vector of length  $n$  with the probability density function  $z = \frac{1}{\sigma\sqrt{2\pi}} e^{-(x-\mu)^2/2\sigma^2}$  with  $\mu = 0, \sigma = 1$  along with the embedded steel grade. The dimension of the embedding layer  $E(Gr)$  is equal to  $n$ . The architecture of the generator is the following:

- noise = Flatten( $z$  ( $\mu = 0, \sigma = 1$ ))
- label = Flatten(Embedding(Steel Grade))
- product = Multiply(noise, label)
- x1 = LeakyRelu(Dense(product, 256))
- x2 = LeakyRelu(Dense(x1, 128))
- x3 = LeakyRelu(Dense(x2, 64))
- $y$  = Reshape(LeakyRelu(Dense(x3,  $n \cdot \text{seqlength}$ )))

The discriminator shares the same architecture, with the difference that the last layer is a dense layer with one neuron. In fact, we treat the data as if it was a small image, which results in quite a good approximation of sequential properties. The real strips data are standardized before being fed to the discriminator. Then we train either the generator or the discriminator at a time with the weights of the other part frozen, using techniques proven to be helpful in achieving more stability in GAN training, for example label smoothing [22] and training the discriminator on  $k$  times as much data as we give to the generator on each epoch [23]. We use the Adam optimizer [24] and train a model for 2000 epochs. The results are presented in Figure 3. The distribution of the crucial parameters of the rolls is approximated quite well.

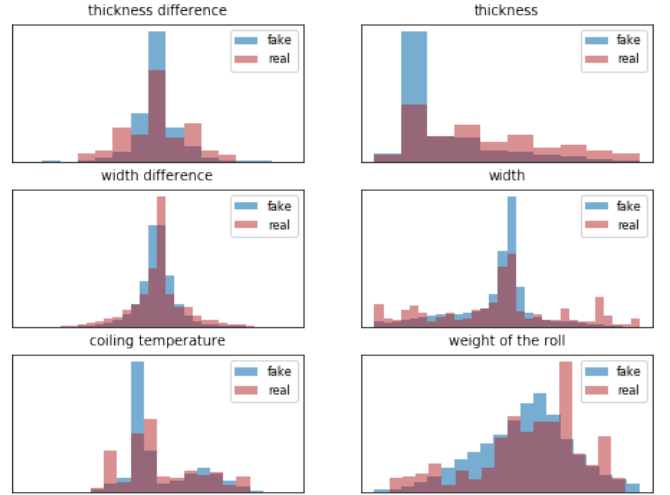


Fig. 3. Comparison of real and generated strips

### C. RL: Model description and parameters choice

To solve our continuous optimization problem in a simple way, we treat it as a sequence of episodic tasks, with the length of an episode limited by 20 consecutive steel strips passed through the kinematic environment described earlier. Therefore, one can transform the objective function to the following:  $\text{maximize } \sum_{i=1}^n v_{s,i}$ , where  $n = \sum_{i=1}^{20} t_{f,i}$ . Meaning the general approach widely accepted for the RL framework we define the following settings: Reward function, State, Policy evaluation strategy and Action.

We exploit a multi-agent approach, when two agents cooperatively define the finally applied action. The resulted action is obtained as a plain sum of actions evaluated by the agents and is determined as the speed of the STU at every time step.

1) *Reward*: Despite the fact that we are using a multi-agent approach, we consider the reward function to be applied only for the second agent (RL-agent). According to the problem description there should be two main contributors to the reward function: a reward associated with an increase in the values of the objective function and penalties acquired from a violation of constrains. In the analytical solution developed for the problem the two contributors have already been accounted.

Therefore, we consider the contribution the RL-agent imposes to the group success or failure relative to the effect acquired from the implementation of the conservative agent solely. We define the reward function of our RL-agent consisting of the following terms: the contribution to the STU's speed with positive sign, the violation of constraints associated with the death of the agent with negative sign and, optionally, the degree of proximity to boundaries of constraints.

2) *State*: The state vector was chosen as follows

$$S_i = (V_{f,i}, V_{s,i}, v_{f,i}, v_{s,i}, v_{t,i}, t_{W,pred}, L_{f,i}, L_{t,i})$$

, where  $t_{W,pred}$  indicates the expected time left to the end of the welding stage (based on the predicted welding time value).

3) *Policy evaluation strategy*: We used Deep Q-learning for the evaluation of the most optimal STU's speed regulation strategy. In Q-learning the action-value (or Q-value) is used to estimate the expected sum of the gamma-discounted rewards acquired from taking action  $a_i$  in state  $s_i$  and yielding reward  $r_{i+1}$  and a subsequent transition to state  $s_{i+1}$ . In terms of *Bellman equation* it could be rewritten for the immediate reward in form [2]:

$$Q(s_i, a_i) \leftarrow Q(s_i, a_i) + \alpha [r_{i+1} + \gamma \max_a Q(s_{i+1}, a) - Q(s_i, a_i)]$$

In Deep Q-learning instead of the scalar Q-value the Q-value function approximation is used with the neural network (NN) as a function approximation technique.

Considering the clear periodicity in the technological routine of the FTU and the TTU attributed with the repetition of even movement, then equidistant movement and final immobility, one can redefine the behaviour of these units in terms of stages. Therefore, one could distinguish three stages: boost ('0'), slowdown ('2') and welding (cutting) ('3'). Meaning the situation when the speed of the FTU or the TTU is forced to speed of the STU at the amount of steel in the hook approaching a certain boundary, one could add an extra synchronisation stage ('1'). Thus, there are sixteen stage combinations. For each combination ( $C^k$ ) we initialized a separate neural network responsive for the Q-value function approximation. Every network takes normalized state values as an input and passes it through the fully-connected network. Every hidden layer of the network is built from neurons with a ReLu activation function and a l1-regularizer. The last linear layer outputs 1-d vector with Q-values associated with available actions, ranged from 1 to 10. While naturally speed is understood as a continuous quantity, in our case the simplification of it to the discrete variable is explained by the controller's regulation abilities.

Switching between different NN could be described as follows, when a new stage combination becomes active the appropriate NN is taken and the Q-value is updated with the reward evaluated from previous steps with the same function approximation network. The update for the function approximation as well as choosing of the appropriate action is done only once at the beginning of a new stage combination and is kept until the next stage combination arrives. The pseudo-code for the entire learning procedure is shown in Algorithm 1

---

**Algorithm 1** Pseudo-code for Q-value function approximation learning

---

```

1: Initialization of kinematic ENV, C-Agent
2: Initialization of NN  $Q(s, a|\theta)$  for every combination  $C^k$ 
3: for episode in range(1, M) do
4:   Receive roll sequence, disturbance parameters
5:   Receive initial state  $s_1$ 
6:   for t in range(1, T) do
7:     if  $C_t^k \neq C_{t-1}^k$  then
8:       Observe state  $s_t^k$  and reward  $r_{t-1}^k$ 
9:       Select action  $a_{t,RLagent}^k$  according to  $\epsilon$ -greedy
           policy from  $Q^k(s_t^k, a_{t-1}^k|\theta)$ 
10:      Select action  $a_{t,C-agent}^k$ 
11:      Receive cumulative action  $a_t^k = a_{t,RLagent}^k +$ 
            $a_{t,C-agent}^k$ 
12:      Set  $z_{t-1} = r_{t-1}^k + \gamma \max_a Q^k(s_t^k, a_{t-1}^k|\theta)$ 
13:      Update weights of NN by minimizing the loss:
            $L(\theta) = \frac{1}{N} \sum_t |z_{t-1} - Q^k(s_{t-1}^k, a_{t-1}^k|\theta)|^2$ 
14:      Update step size  $\alpha$  to reduce on factor 0.003
15:     end if
16:     Execute action  $a^k$  and observe state  $s_{t+1}$ 
17:     Update reward  $r^k$  until stage combination ends
18:     if constraints were violated then
19:       break
20:     end if
21:   end for

```

---

4) *Action, cooperation strategy*: Next, we introduce two RL-agents with several different key points in respect to their interaction with the conservative agent, while the architecture of the solution stays the same.

We explore the behavior of two RL-agents, since they represent the different approach to the final solution. On the one hand, we consider a fully cooperative agent (*F-Coop Agent*), when the decision on the action applied to the system is assessed by both agents at every change of the stage combination. On the other hand, we describe a more conservative but more industry tolerated agent (*P-Coop Agent*), where the cooperative decision is taken for all stage combinations except those where the welding or cutting stage is involved. That is done, because the duration of these stages is not well defined and any lapses in logic may result in continuous downtime of the pickling line.

The variations in the earlier introduced solution done for every agent are shown in Table II. The modified parameters are the number of layers in NNs responsive for the Q-value approximation, the composition of the state vector, the reward function evaluation strategy, the range of available actions and the frequency of actions selection.

#### IV. RESULTS AND DISCUSSION

The agents were firstly trained at 800 episodes with generated initial conditions (IC) and  $\epsilon$ -greedy policy. Then  $\epsilon$  was forced to zero and the training was continued to the next 200

TABLE II  
SETTING'S VARIATIONS FOR RL-AGENTS

Parameter	<i>P-Coop Agent</i>	<i>F-Coop Agent</i>
The number of NNs layers	2 (8 — 8)	3 (32 — 64 — 16)
The state vector	$(V_{f,i}, V_{s,i}, v_{f,i}, v_{t,i}, t_{W,pred}, L_{f,i}, L_{t,i})$	$(V_{f,i}, V_{s,i}, t_{W,pred}, L_{f,i}, L_{t,i})$
The reward contributors	(action, constraints violation)	(action, constraints violation, proximity to boundaries of constrains)
The reward on stage calculation ( $t'$ - stage combination duration)	$\sum_{i=1}^{t'} r_i$	$\frac{1}{t'} \sum_{i=1}^{t'} r_i$
Action from agent	[0, 9]	[-5, 5]
Frequency	Every stage combination, except where welding or cutting stage is involved	Every stage combination, plus every 30 sec. during combination time

episodes with the IC taken from the historical data. All the IC and states were precomputed to ensure the re-productivity and identity of the starting condition for different agents. For generated IC the pipeline shown in Figure 2 was used. Below, the results obtained at the last 100 episodes with historical IC are discussed.

Above we have determined the objective function of our problem as a sum of the STU speeds obtained at every time step during the episode. With the limitation of the episode to the production time of 20 consecutive steel stripes one could redefine the objective function as an average STU speed per episode. In Figure 4 the results for the original objective function as well as for the modified one (average speed) are shown. Here and further we distinguish the *C-Agent* applied stand-alone as a baseline solution to compare the gain in productivity arising from the implication of the RL-approach and *C-Agent per stage* as an agent that contributes to the decision made by the RL-agent. The *C-Agent*, as a baseline solution, acts every second, while the RL-agents are more restricted in the acting frequency (see Table II).

As it is seen from Figure 4 the decision on which the agent shows the best strategy depends on the approach taken for the objective function. The *F-Coop Agent* shows the best performance if an average speed is considered as a decision function and significantly loses when the sum of speed per episode is assessed. Such behavior could be explained by the rate of agents death. The early death of the agent results in shortening of the episode length, while its effect to the average speed is not obvious and even may result in an increase in the average speed value.

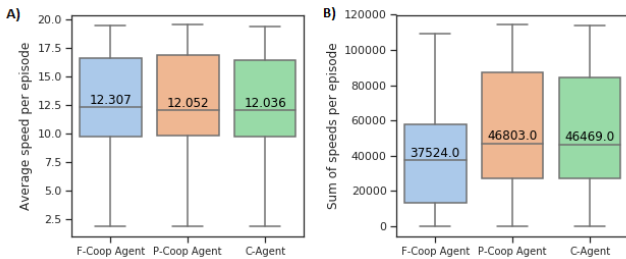


Fig. 4. Objective function for *F-Coop Agent*, *P-Coop Agent* and *C-Agent* agents. A) Average STU speed per episode; B) Sum of STU speed during the episode. Values shown in boxes correspond median values of distributions.

In Table III the rate of agents death is presented with the differentiation for the stage combination when the death happened. Logically, most of the deaths occurred at the stage combinations when either welding or cutting stage('3') took place. These stages possess a high variability in the duration time and while this time could be predicted with some errors the agents hardly adapted to such variations. Moreover, some deaths could be described by starting conditions, when the initiation took place at a stage combination with welding or cutting stage involved, a death could be expected with a high probability. Nevertheless, the comparison of the excessive death rate of the RL-agents (Fully Cooperative and Partly Cooperative) over the *C-Agent* (27% death rate) shows a significant growth of deaths rate for *F-Coop Agent* (43% death rate) over the *P-Coop Agent* (26% death rate). These data also confirm the assumption done from the objective function consideration, that lower values of the speed's sum for *F-Coop Agent* as well as for *C-Agent* could be attributed to a higher death rate.

TABLE III  
DEATH RATE FOR DIFFERENT AGENTS

Agents	Stage combinations								
	01	03	10	13	23	30	31	32	33
<i>F-Coop Agent</i>	5	3	1	6	0	3	2	2	22
<i>P-Coop Agent</i>	0	1	1	2	1	2	1	2	15
<i>C-Agent</i>	0	1	1	2	1	2	2	2	15

Stage combinations: 'stage in FTU' + 'stage in TTU'

To clarify the reasons for the excessive death rate the comparison of the speed taken by the agents with the speed contributed by *C-Agent per stage* for every stage combination is presented in Figure 5. Since we know that most of the death is associated with having-'3' combinations we could take a more close look at them. According to the initial descriptions of the agents, the *P-Coop Agent* is restricted at having-'3' stages by the decision made by *C-Agent per stage*. Therefore, there is only a minor deviation, less than 3.5%, of the entire speed displayed by the agent over the basic decision of *C-Agent per stage* (Figure 5 (B)). Meanwhile, the *F-Coop Agent* could act with positive or negative additive over the base decision of *C-Agent per stage*. As it is shown in Figure 5 (A) the final action taken by *F-Coop Agent* in having-'3' stages



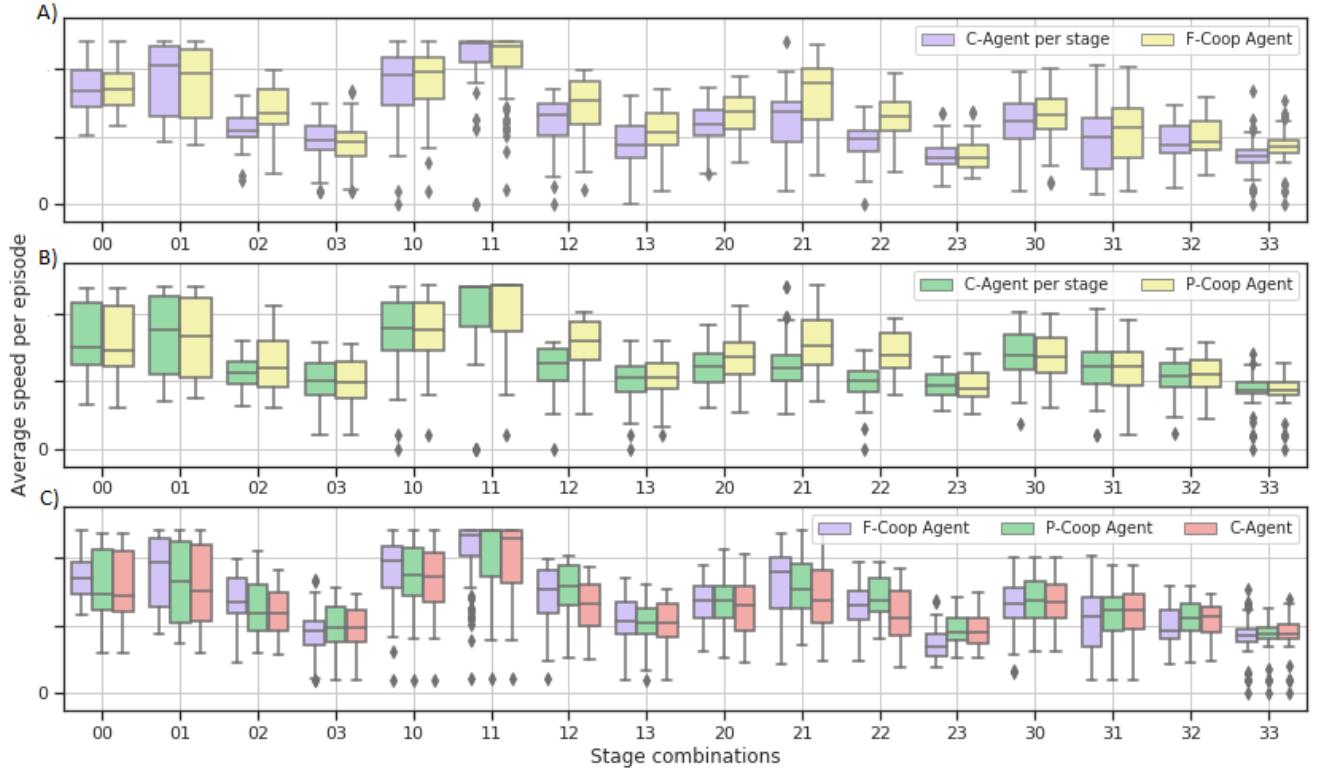


Fig. 5. Objective function for Fully Cooperative, Partly Cooperative and Conservative agents. A) Average STU speed per episode; B) Sum of STU speed during the episode.

exceeds the speed suggested by *C-Agent per stage* in most of the cases. Thus, from 7 having-'3' stages in 5 of them we detect a surplus, and in 3 of them the surplus is over 15% of the basic decision of *C-Agent per stage*. The reason why the *F-Coop Agent* gives an excess for having-'3' stages in spite of the high death rate for such stages lies in the dynamic control system of the pickling line. There is a preventing save system that forces the speed of the STU down when the line approaches to critical conditions. The influence of that system is short but for some cases it helps to avoid a potential death. Therefore, such environment promotes the agent to set the speed at having-'3' stages high enough and believes that the preventing save system will save it later on from death.

Besides the having-'3' stages, the excess in speed of the agents over the speed suggested by *C-Agent per stage* occurred also for having-'2' stages. In Table IV the surplus as the percentage of the base agent speed is calculated. Both agents, *F-Coop Agent* and *P-Coop Agent* show identical behavior that could be attributed to the potentially positive effect of the RL-approach. In Figure 5 (C) the final results of the comparison of the speeds from *F-Coop Agent*, *P-Coop Agent* and *C-Agent* are presented. The same tendency for having-'2' stages is preserved here, we detect a distinct excess of the RL-agents speed over the conservative *C-Agent*, although it is less pronounced than in the case of *C-Agent per stage*. Therefore, we could consider it as the main effect of the application of

the RL-agents to the current problem.

TABLE IV  
SPEED EXCESS OF RL-AGENTS IN PERCENT OVER THE CONSERVATIVE AGENT

Agents	Stage combinations				
	02	12	20	21	22
<i>F-Coop Agent vs. C-Agent per stage</i>	23	17	16	30	36
<i>F-Coop Agent vs. C-Agent</i>	14	17	6	31	18
<i>P-Coop Agent vs. C-Agent per stage</i>	7	26	12	27	35
<i>P-Coop Agent vs. C-Agent</i>	1	21	6	12	25

Stage combinations: 'stage in FTU' + 'stage in TTU'

From all of the above we could conclude that while *F-Coop Agent* shows sometimes better STU speed values than *P-Coop Agent* and could be considered as a more flexible agent, its risky decisions are responsible for a higher death rate and therefore for a lower value of the objective function. At the same time, the more conservative *P-Coop Agent* allows the increase in speed of the STU only in safe condition and thereby results in a higher productivity.

## V. CONCLUSIONS

In this work, we have proposed a multi-level approach addressed to the productivity problem on a metallurgical pickling line. At the first level, the combination of LSTM and CGAN has been exploited to generate the realistic input

data and thereby to overwhelm the deficiency in original data necessary to solve the problem. Then several steps have been done, that only partially described in the manuscript, such as development of C-agent based on the analytical solution of the problem and the kinematic environment simulating the real processes on the pickling line. Finally, at the third level the complete architecture of the Multi-Agent Reinforcement Learning system has been built and trained. The entire approach with *P-Coop Agent* involved has been successfully applied at the Cherepovets Steel Mill and has allowed to increase the productivity of the pickling line by more than 5% and to significantly improve line automation processes.

#### ACKNOWLEDGMENT

The authors wish to thank the Flat Rolled Products Subdivision at the Cherepovets Steel Mill and especially Andrei Fedotov and Alexandr Ruban for valuable knowledge and assistance during the project.

#### REFERENCES

- [1] H. Ahuett-Garza and T. Kurfess, "A brief discussion on the trends of habilitating technologies for industry 4.0 and smart manufacturing," *Manufacturing Letters*, vol. 15, pp. 60–63, 2018.
- [2] R. S. Sutton and A. G. Barto, *Reinforcement learning: An introduction*. Cambridge, MA: MIT Press, 2011.
- [3] O. Gottesman, F. Johansson, J. Meier, J. Dent, D. Lee, S. Srinivasan, L. Zhang, Y. Ding, D. Wihl, X. Peng *et al.*, "Evaluating reinforcement learning algorithms in observational health settings," *arXiv preprint arXiv:1805.12298*, 2018.
- [4] S. Chakraborty, "Capturing financial markets to apply deep reinforcement learning," *arXiv preprint arXiv:1907.04373*, 2019.
- [5] I. Arel, C. Liu, T. Urbanik, and A. G. Kohls, "Reinforcement learning-based multi-agent system for network traffic signal control," *IET Intelligent Transport Systems*, vol. 4, no. 2, pp. 128–135, 2010.
- [6] R. Nian, J. Liu, and B. Huang, "A review on reinforcement learning: Introduction and applications in industrial process control," *Computers & Chemical Engineering*, p. 106886, 2020.
- [7] J. B. Tytus, "Metal-pickling process," Jun. 30 1925, uS Patent 1,544,506.
- [8] P. Priore, D. De La Fuente, A. Gomez, and J. Puente, "A review of machine learning in dynamic scheduling of flexible manufacturing systems," *Ai Edam*, vol. 15, no. 3, pp. 251–263, 2001.
- [9] A. Xanthopoulos, D. Koulouriotis, and A. Gasteratos, "A reinforcement learning approach for production control in manufacturing systems," in *1st International Workshop on Evolutionary and Reinforcement Learning for Autonomous Robot Systems, ERLARS*. Citeseer, 2008, pp. 33–40.
- [10] W. Daosud, P. Thitiyasook, A. Arpornwichanop, P. Kittisupakorn, and M. A. Hussain, "Neural network inverse model-based controller for the control of a steel pickling process," *Computers & Chemical Engineering*, vol. 29, no. 10, pp. 2110–2119, 2005.
- [11] P. Kittisupakorn, P. Thitiyasook, M. A. Hussain, and W. Daosud, "Neural network based model predictive control for a steel pickling process," *Journal of process control*, vol. 19, no. 4, pp. 579–590, 2009.
- [12] I. J. Goodfellow, J. Pouget-Abadie, M. Mirza, B. Xu, D. Warde-Farley, S. Ozair, A. Courville, and Y. Bengio, "Generative adversarial nets," in *Proceedings of the 27th International Conference on Neural Information Processing Systems - Volume 2*, ser. NIPS14. Cambridge, MA, USA: MIT Press, 2014, p. 26722680.
- [13] A. Radford, L. Metz, and S. Chintala, "Unsupervised representation learning with deep convolutional generative adversarial networks," *arXiv preprint arXiv:1511.06434*, 2015.
- [14] H. Shangguan and R. Mukundan, "3d human pose dataset augmentation using generative adversarial network," in *Proceedings of the 2019 3rd International Conference on Graphics and Signal Processing*, ser. ICGSP 19. New York, NY, USA: Association for Computing Machinery, 2019, p. 5357. [Online]. Available: <https://doi.org/10.1145/3338472.3338475>
- [15] J. Yoon, D. Jarrett, and M. van der Schaar, "Time-series generative adversarial networks," in *Advances in Neural Information Processing Systems*, 2019, pp. 5509–5519.
- [16] C. Donahue, J. McAuley, and M. Puckette, "Adversarial audio synthesis," *arXiv preprint arXiv:1802.04208*, 2018.
- [17] C. Vondrick, H. Pirsiavash, and A. Torralba, "Generating videos with scene dynamics," in *Advances in neural information processing systems*, 2016, pp. 613–621.
- [18] Z. Che, Y. Cheng, S. Zhai, Z. Sun, and Y. Liu, "Boosting deep learning risk prediction with generative adversarial networks for electronic health records," *IEEE*, 2017, pp. 787–792.
- [19] L. Xu and K. Veeramachaneni, "Synthesizing tabular data using generative adversarial networks," *arXiv preprint arXiv:1811.11264*, 2018.
- [20] L. Xu, M. Skoularidou, A. Cuesta-Infante, and K. Veeramachaneni, "Modeling tabular data using conditional gan," in *Advances in Neural Information Processing Systems*, 2019, pp. 7333–7343.
- [21] S. Hochreiter and J. Schmidhuber, "Long short-term memory," *Neural computation*, vol. 9, no. 8, pp. 1735–1780, 1997.
- [22] T. Salimans, I. Goodfellow, W. Zaremba, V. Cheung, A. Radford, and X. Chen, "Improved techniques for training gans," in *Advances in neural information processing systems*, 2016, pp. 2234–2242.
- [23] I. Goodfellow, "Nips 2016 tutorial: Generative adversarial networks," *arXiv preprint arXiv:1701.00160*, 2016.
- [24] D. P. Kingma and J. Ba, "Adam: A method for stochastic optimization," *arXiv preprint arXiv:1412.6980*, 2014.